

Synthesis of Sn doped CuO nanotubes from core–shell Cu/SnO₂ nanowires by the Kirkendall effect

This article has been downloaded from IOPscience. Please scroll down to see the full text article.

2010 Nanotechnology 21 295601

(<http://iopscience.iop.org/0957-4484/21/29/295601>)

View [the table of contents for this issue](#), or go to the [journal homepage](#) for more

Download details:

IP Address: 152.3.196.116

The article was downloaded on 27/08/2010 at 21:19

Please note that [terms and conditions apply](#).

Synthesis of Sn doped CuO nanotubes from core–shell Cu/SnO₂ nanowires by the Kirkendall effect

Min Lai¹, Syed Mubeen², Nicha Chartuprayoon²,
Ashok Mulchandani², Marc A Deshusses³ and Nosang V Myung^{2,4}

¹ School of Mathematics and Physics, Nanjing University of Information Science & Technology, Nanjing 210044, People's Republic of China

² Department of Chemical and Environmental Engineering and Center for Nanoscale Science and Engineering, University of California–Riverside, Riverside, CA 92521, USA

³ Department of Civil and Environmental Engineering, Duke University, Box 90287, Durham, NC 27708, USA

E-mail: myung@engr.ucr.edu

Received 2 April 2010, in final form 1 June 2010

Published 29 June 2010

Online at stacks.iop.org/Nano/21/295601

Abstract

Sn doped CuO nanotubes were synthesized by thermal oxidization of Cu/SnO₂ core–shell nanowires in air through the Kirkendall effect. The Cu/SnO₂ core–shell nanowires were sequentially electrodeposited by forming a SnO₂ shell followed by electrodeposition of the Cu core. After thermal treatment in air, the core–shell Cu/SnO₂ (13 ± 2 nm thick shell on 128 ± 15 nm in diameter core) nanowires were oxidized to form Sn doped CuO nanotubes with an average wall thickness and outer diameter of 54 nm and 176 nm, respectively. Room temperature *I*–*V* characterization indicated that the electrical resistivity of the nanostructures was 870 ± 85 Ω cm. The methodology that was demonstrated is very general and could be used to synthesize coaxial SnO₂ shells with a variety of electrodeposited cores. In addition, doped metal oxide nanotubes can be readily synthesized by thermal oxidization of core–shell nanowires in air where the dopant content can be tuned by controlling the shell thickness through adjusting the deposition time.

(Some figures in this article are in colour only in the electronic version)

1. Introduction

Cupric oxide (CuO) is an important p-type semiconducting material with an indirect band gap (E_g) of 1.0–2.08 eV [1, 2]. In particular, owing to their size-dependent properties and unique structures, one-dimensional (1D) cupric oxide (CuO)-based nanostructures have attracted intense scientific interest with potential applications in heterogeneous catalysis, lithium batteries, solar energy conversion, high-temperature superconductivity, chemical and biological sensing, and field emission [1, 3–6]. A variety of physical and chemical techniques have been employed to form 1D CuO nanostructures including thermal evaporation, thermal decomposition, thermal oxidation, electrospinning, solid–liquid arc discharge processes, chemical vapor deposition, anodization,

templating routes, sol–gel methods, and hydrothermal or solvothermal treatments [7–14]. The properties of CuO-based nanostructures can be tuned by forming heterostructures and composites or doping [15–18]. However, little effort has been placed in synthesizing doped CuO nanostructures.

The Kirkendall effect is a classical phenomenon in materials sciences, in which atomic diffusion is by a vacancy mechanism. The Kirkendall effect was first applied at the nanoscale to form hollow cobalt oxide and chalcogenide nanocrystals by Yin *et al* [19]. Such an effect has also been extended to fabricate various hollow nanoparticles and nanotubes [20–25] where diffusivity, reaction temperature, and concentration profile control the morphology of the nanostructures [20, 26, 27].

In this work, we employed a template-directed electrodeposition route to first synthesize coaxial Cu/SnO₂ core–shell

⁴ Author to whom any correspondence should be addressed.

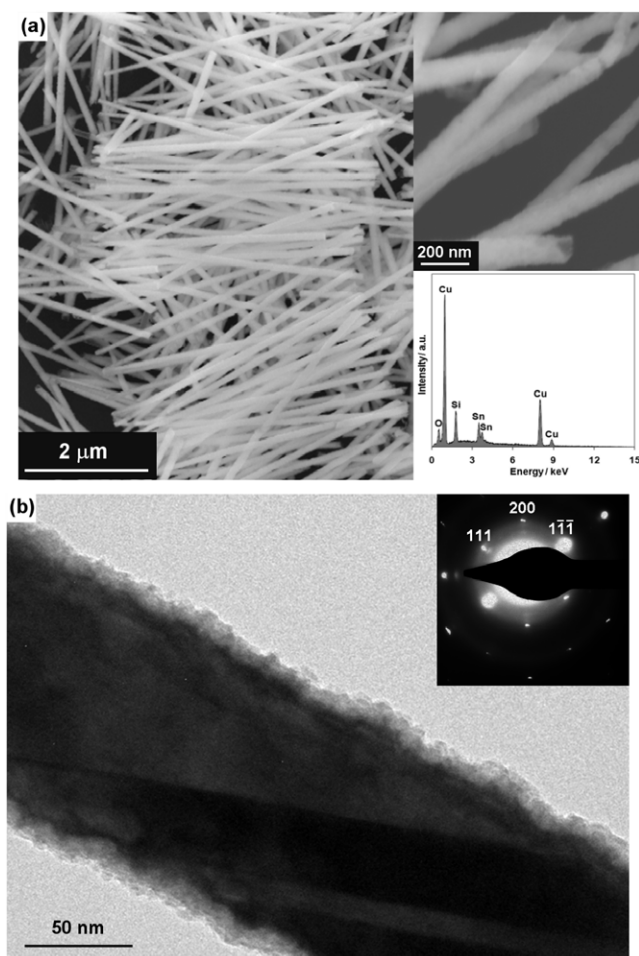


Figure 1. (a) FE-SEM images of the as-prepared Cu/SnO₂ core-shell nanowires. The insets show a higher magnification and the corresponding EDS spectrum. (b) TEM image of the as-prepared Cu/SnO₂ core-shell nanowires. The inset is the corresponding SAED pattern.

nanowires. Sn doped CuO nanotubes were then formed after annealing the Cu/SnO₂ core-shell nanowires in air.

2. Experimental details

Cu/SnO₂ core-shell nanowires were first formed via a two-step process including template-directed electrodeposition of SnO₂ nanotubes and a further electrodeposition of a metallic copper core within the as-grown SnO₂ nanotubes. In both electrodepositions, platinum gauze was used as the counter electrode and a Ag/AgCl (3 M KCl) electrode served as the reference electrode. Electrochemical synthesis was performed under potentiostatic mode using a VMP2 multichannel potentiogalvanostat (Bio-Logic LLC, Knoxville, TN). The procedure for the synthesis of a SnO₂ shell has been described in detail elsewhere [28]. Briefly, SnO₂ shells were electrochemically synthesized using nuclear track etch polycarbonate membranes (Whatman Nuclepore[®]) with a nominal pore diameter of 50 nm. The rated membrane thickness and pore density were approx. 6 μm and 6 × 10⁸ pores cm⁻², respectively. One side of the polycarbonate

membrane was first coated with a 500 nm thick layer of gold by sputtering (Emitech K500X table-top sputter, UK), to create a seed layer. The electrical contact was made to the membrane working electrode using conductive copper tape. The resultant template was placed in an electrolyte cell such that an area of 1 cm² was exposed to the electrolyte. The electrolyte consisted of 20 mM tin chloride, 0.1 M sodium nitrate, and 75 mM nitric acid in nanopure (>18 MΩ cm⁻¹) water. SnO₂ was deposited in the template using a fixed potential of -0.4 V (versus Ag/AgCl reference electrode) for 2 h. Copper core electrodeposition was performed in an aqueous electrolyte solution containing 0.2 M CuSO₄ and 0.1 M H₃BO₃ with a constant potential of -0.2 V (versus the Ag/AgCl reference electrode) for 1 h. After deposition, the gold layer used as the working electrode was mechanically removed and the membrane was rinsed in deionized water. The nanostructures were released by dissolving the polycarbonate membrane in 10 ml dichloromethane. The suspension was centrifuged and the nanostructures were washed three times with 1 ml dichloromethane and finally suspended in 0.5 ml isopropanol. To form Sn doped CuO nanotubes, the Cu/SnO₂ core-shell nanowires were thermally oxidized in air at 400 °C for 4 h. All chemicals were analytical grade which were purchased from Fisher Scientific, Inc.

Field emission scanning electron microscope (FE-SEM) images and energy-dispersive x-ray spectra (EDS) were obtained using a Philips XL30 FEG SEM microscope operated at 15 kV. Transmission electron microscope (TEM) images, high resolution TEM (HR-TEM) images and selected area electron diffraction (SAED) patterns were recorded on a FEI-Philips CM300 microscope operated at 300 kV. The electrodes for the temperature-dependent resistance were microfabricated by coating (100) oriented silicon wafers with 1 μm thick SiO₂ film by CVD, photo-lithographically defining the electrode area, evaporating a 20 nm thick Cr adhesion layer and a 300 nm thick Au layer and finally defining the electrodes using lift-off techniques. The gap distance between the electrodes was fixed at 3 μm. Sn doped CuO nanotubes were assembled on the electrodes by AC dielectrophoretic alignment with the peak-to-peak voltage of 20 V and frequency of 1 MHz, using suspensions in dimethyl formamide (DMF) [29]. Temperature-dependent electrical resistance (TCR) was determined using a Keithley 236 source-measure unit and a cryogenic cooling system.

3. Results and discussion

The electrochemical assisted synthesis of SnO₂ in templates has been investigated by our group [28, 30]. In acidic electrolyte solution, hydrogen ions are consumed during the electrochemical reduction of nitrate ions. The increase of the local pH in the presence of tin ions leads to the precipitation of tin dioxide in template channels. FE-SEM images of coaxial Cu/SnO₂ core-shell nanowires are displayed in figure 1(a). The statistical result yields an average length of 5.4 μm and a standard deviation of 0.4 μm (8%). The relative standard deviation in length is much smaller than that of SnO₂ nanotubes (33%) without a copper core [28]. The

explanation for this difference may lie in the structure of the nanomaterials. In the core-shell nanowire structure, the copper core improves the ductility and strength of the nanowires and results in less damage during the template removal and washing processes. The SnO₂ nanotubes in the absence of the core were mechanically weak due to the thin tube walls (less than 20 nm) and brittle nature of metal oxides. Higher magnification of the core-shell Cu/SnO₂ nanowires (top inset in figure 1(a)) shows unfilled nanotube tips, indicating the copper core is entirely covered by the SnO₂ shell. It also indicates that the formation of the copper core was a bottom-up growth process and the conductivity of as-grown SnO₂ tube walls was poor before the crystallinity was enhanced via the annealing process. TEM images also confirmed this finding (figure 1(b)). The EDS spectrum (bottom inset figure 1(a)) shows the presence of Cu, Sn and O peaks with an atomic ratio of tin to copper of 6/94.

Examination of the TEM image reveals that the core-shell nanowires possess a uniform SnO₂ shell with a thickness of 13 ± 2 nm, which is thinner than the walls of pure SnO₂ nanotubes (24 ± 2 nm) synthesized using the same templates [28]. The diameter of the core-shell nanowires (128 ± 15 nm) is slightly larger than that of SnO₂ nanotubes (103 ± 13 nm) without copper core. These differences can be attributed to the introduction of the copper core which might compress the SnO₂ shell. The corresponding SAED pattern (inset figure 1(b)) is consistent with the cubic structure of copper, indicating that the copper core is a single crystal.

Figures 2(a) and (b) show the morphology of the Sn doped CuO nanotubes after thermal oxidation in air at 400 °C for 4 h. The bright field (BF)-TEM image (figure 2(b)) clearly shows the formation of a tubular structure with an average internal diameter of 69 ± 8 nm. The corresponding SAED pattern (inset figure 2(b)), and dark field (DF)-TEM image (figure 2(b) inset) reveal the polycrystalline nature of the thermally oxidized products. The SAED pattern is consistent with polycrystalline monoclinic CuO structures, indicating that CuO nanotubes were formed via the oxidation of the Cu cores. Figure 2(c) shows the HR-TEM image of annealed Sn doped CuO nanotubes and the distance of the marked fringes which is consistent with interplanar spacing of the monoclinic CuO{110} planes.

Figure 3 shows histograms of the diameter distribution of the Sn doped CuO nanotubes after the annealing process. It is apparent that the diameter of the nanotubes increased after thermal oxidation. The mean diameter was 128 nm and 176 nm for the as-prepared and annealed samples, respectively. The formation of the tubular structures after thermal oxidation can be attributed to the Kirkendall effect (figure 4) by which atoms exchange with vacancies. At the beginning of the thermal oxidation process, at the interface between Cu and SnO₂, Cu diffused outward whereas oxygen diffused inward. The outward diffusion of Cu is much faster than the inward diffusion of oxygen which generated vacancies during oxidation [20, 31]. The formation of the hollow structures during the thermal oxidation of Cu/SnO₂ core-shell nanowires indicates that the SnO₂ shell does not significantly affect the diffusion of copper and oxygen.

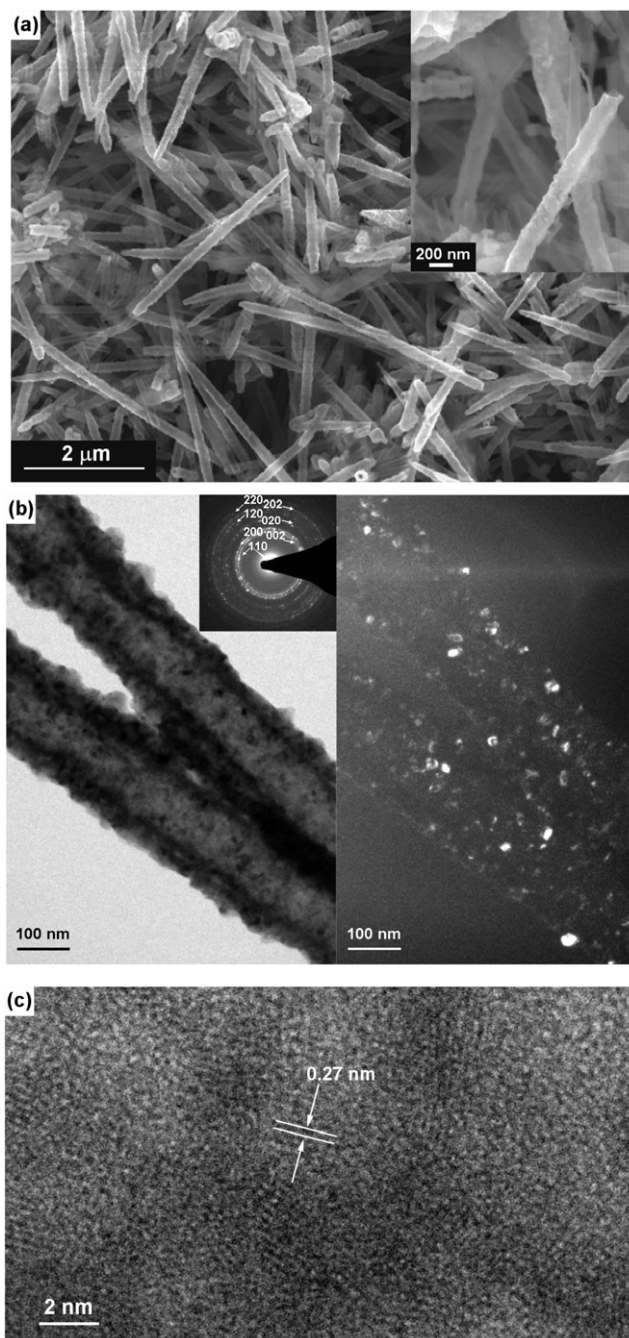


Figure 2. Sn doped CuO nanotubes: (a) FE-SEM images and higher magnification (inset); (b) BF-(left) and DF-(right) TEM images and corresponding SAED pattern (inset); (c) HR-TEM image.

The electrical properties of the Sn doped CuO nanotubes were investigated by performing I - V measurements at a series of temperatures from 30 to 295 K. Three typical I - V curves are displayed in figure 5. The nonlinear curves indicate that the electrical characteristics follow Schottky barriers between the Sn doped CuO nanotube and Au electrodes. The resistivity of the nanotubes is approximately $(870 \pm 85) \Omega \text{ cm}$ in air at 295 K. The Arrhenius plot of TCR of the nanotubes is shown in figure 5 inset. For semiconducting materials, the electrical

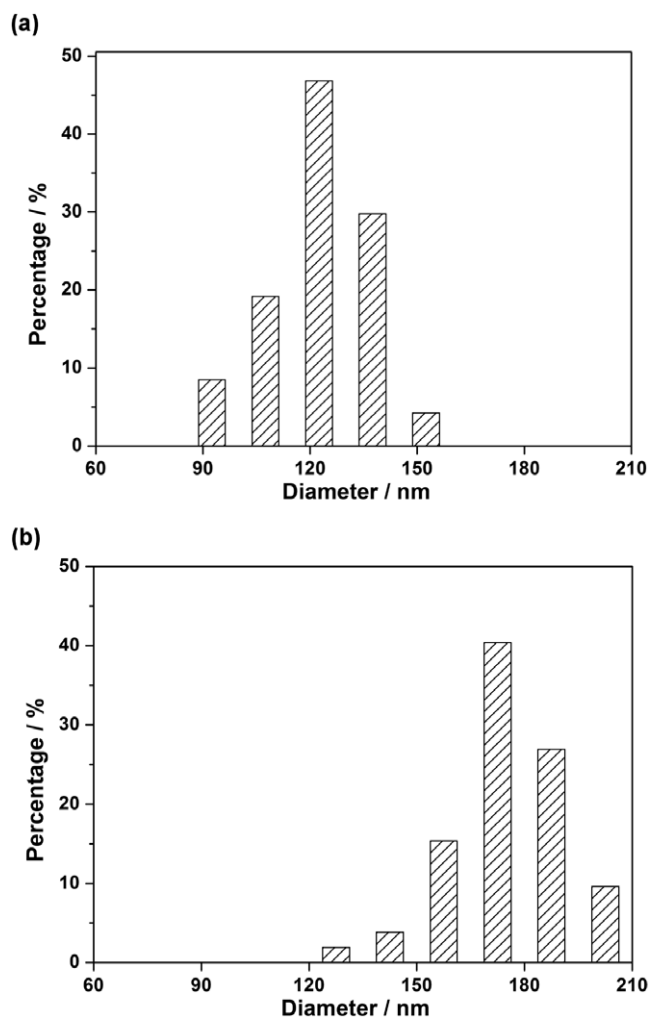


Figure 3. Histograms of the diameter distribution of the Cu/SnO₂ core-shell nanowires (a) and tin doped CuO nanotubes (b).

resistance (R) can be described by:

$$R(T) = R_0 \exp(E_A/k_B T) \quad (1)$$

where T , k_B , E_A and R_0 are the temperature, the Boltzmann constant, the activation energy and the pre-exponential factor, respectively [32]. The plot in figure 5 inset shows two linear regions. By linear fitting in those two regions, two activation energy values, (113 ± 11) meV (E_{A1}) and (2.1 ± 0.3) meV (E_{A2}), are obtained for temperatures above and

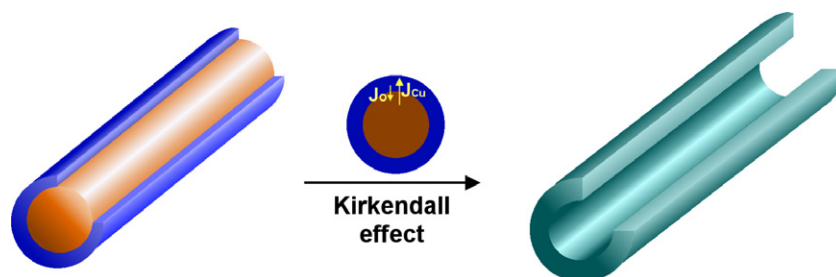


Figure 4. Schematic illustration of the formation of a nanotube by the Kirkendall effect. Parts of the shell and the tube wall are neglected to reveal the internal structures.

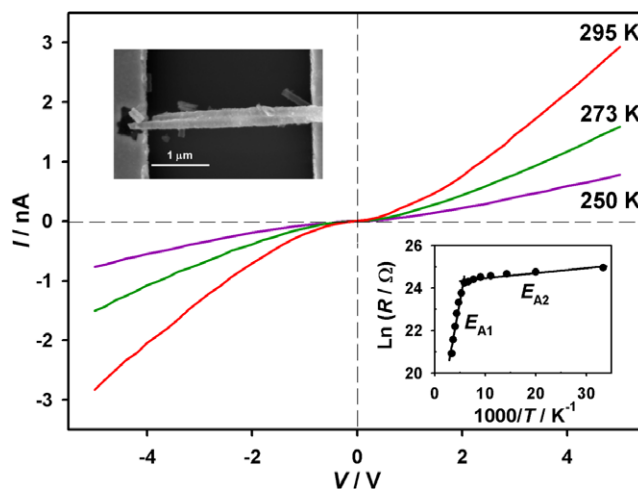


Figure 5. Typical I - V curves of the Sn doped CuO nanotubes measured at 295, 273 and 250 K. The insets are the SEM image of the Sn doped CuO nanotube aligned across gold electrodes using AC dielectrophoresis alignment and the Arrhenius plot of temperature-dependent resistance.

below 170 K, respectively. The activation energy, E_{A1} , obtained above 170 K may be attributed to the ionization energy of the main donor centers. At temperatures below 170 K, the nanotube resistance is weakly dependent on the temperature which indicates that a different conduction mechanism is dominant. Modest variations of the resistance at low temperatures have also been observed for CdTe thin films [33] and nanowires [34], ZnO [35] and GaN [36, 37] nanowires and SnO₂ nanotubes [28]. This observation can be explained by the fact that the electrical conduction comes from carriers hopping from impurity levels. The transition temperature of the impurity band conduction is approximately 170 K. Such impurity states can be associated with defects located either in the bulk or on the surface of the nanotubes.

4. Conclusion

In summary, we demonstrated that coaxial Cu/SnO₂ core-shell nanowires were synthesized by template-directed electrodeposition and Sn doped CuO nanotubes were formed after thermal oxidation of the core-shell nanowires in air through the Kirkendall effect. The coaxial Cu/SnO₂ core-shell nanowires had a Cu core with a diameter of $128 \pm$

15 nm and a thin SnO₂ shell with a thickness of 13 ± 2 nm. The methodology that was demonstrated is very general and it is envisaged that it can be extended to generate coaxial SnO₂-shelled materials with various electrodeposited cores. After thermal oxidation in air, the core-shell nanowires were oxidized to Sn doped CuO nanotubes with internal and external diameters of 69 and 176 nm, respectively. The *I*-*V* measurements showed that the resistivity of the nanotube was 870 Ω cm in air at 295 K. The temperature dependency of the electrical resistance was investigated. Two dominant mechanisms were attributed to the electrical conduction above and below 170 K, respectively. Sn doped CuO nanotubes may offer promising applications in 1D nanostructure-based devices such as nano gas sensors.

Acknowledgments

This material is based on research sponsored by the National Institute of Environmental Health Sciences under agreement number (grant No. U01ES016026) and National Natural Science Foundation of China (NSFC, No. 20907021). The United States government is authorized to reproduce and distribute reprints for government purposes, not withstanding any copyright notation thereon.

References

- [1] Jun J, Jin C, Kim H, Park S and Lee C 2009 *Appl. Surf. Sci.* **255** 8544
- [2] Hao Y and Gong H 2008 *Chem. Vapor Depos.* **14** 9
- [3] Anandan S, Wen X G and Yang S H 2005 *Mater. Chem. Phys.* **93** 35
- [4] Wang X, Hu C, Liu H, Du G, He X and Xi Y 2010 *Sensors Actuators B* **144** 220
- [5] Aygün S and Cann D 2005 *Sensors Actuators B* **106** 837
- [6] Li C, Wei W, Fang S, Wang H, Zhang Y, Gui Y and Chen R 2010 *J. Power Sources* **195** 2939
- [7] Huang L S, Yang S G, Li T, Gu B X, Du Y W, Lu Y N and Shi S Z 2004 *J. Cryst. Growth* **260** 130
- [8] Wang W, Zhan Y, Wang X, Lui Y, Zheng C and Wang G 2002 *Mater. Res. Bull.* **37** 1093
- [9] Wang H, Xu J Z, Zhu J J and Chen H Y 2002 *J. Cryst. Growth* **244** 88
- [10] Xu J F, Ji W, Shen Z X, Tang S H, Ye X R, Jia D Z and Xin X Q 1999 *J. Solid State Chem.* **147** 516
- [11] Xu G, Liu Y, Xu G and Wang G 2002 *Mater. Res. Bull.* **37** 2365
- [12] Yu T, Zhao X, Shen Z X, Wu Y H and Su W H 2004 *J. Cryst. Growth* **268** 590
- [13] Jiang X C, Herricks T and Xia Y N 2002 *Nano Lett.* **2** 1333
- [14] Xu C H, Woo C H and Shi S Q 2004 *Chem. Phys. Lett.* **399** 62
- [15] Baek K-K and Tuller H L 1993 *Sensors Actuators B* **13** 238
- [16] Hung C-M 2009 *Power Technol.* **196** 56
- [17] Yu J H and Choi G M 2001 *Sensors Actuators B* **75** 56
- [18] Prabhakaran D and Boothroyd A T 2003 *J. Cryst. Growth* **250** 77
- [19] Yin Y, Rioux R M, Erdonmez C K, Hughes S, Somorjai G A and Alivisatos A P 2004 *Science* **304** 711
- [20] Fan H J, Gösele U and Zacharias M 2007 *Small* **3** 1660
- [21] Sun Y and Xia Y 2002 *Science* **298** 2176
- [22] Gao J H, Zhang B, Zhang X X and Xu B 2006 *Angew. Chem. Int. Edn* **45** 1220
- [23] Wang Y, Cai L and Xia Y 2005 *Adv. Mater.* **17** 473
- [24] Fan H J, Knez M, Scholz R, Nielsch K, Pippel E, Hesse D, Zacharias M and Gösele U 2006 *Nat. Mater.* **5** 627
- [25] Zhou J, Liu J, Wang X D, Song J H, Tummala R, Xu N S and Wang Z L 2007 *Small* **3** 622
- [26] Yin Y, Erdonmez C K, Cabot A, Hughes S and Alivisatos A P 2006 *Adv. Funct. Mater.* **16** 1389
- [27] Prasad S and Paul A 2007 *Appl. Phys. Lett.* **90** 233114
- [28] Lai M, Lim J-H, Mubeen S, Rheem Y, Mulchandani A, Deshusses M A and Myung N V 2009 *Nanotechnology* **20** 185602
- [29] Lim J H, Phiboolsirichit N, Mubeen S, Rheem Y, Deshusses M A, Mulchandani A and Myung N V 2010 *Electroanalysis* **22** 99
- [30] Lai M, Martinez J A G, Grätzel M and Riley D J 2006 *J. Mater. Chem.* **16** 2843
- [31] Nakamura R, Tokozakura D, Nakajima H, Lee J G and Mori H 2007 *J. Appl. Phys.* **101** 074303
- [32] Willams W 1902 *Phil. Mag. Series 6* **3** 515
- [33] Moesslein J, Lopez-Otero A, Fehrenbruch A, Kim D and Bube R H 1993 *J. Appl. Phys.* **73** 8359
- [34] Kum M C, Yoo B Y, Rheem Y W, Bozhilov K N, Chen W, Mulchandani A and Myung N V 2008 *Nanotechnology* **19** 325711
- [35] Tazlaoanu C, Ion L, Enculescu I, Sima M, Enculescu M, Matei E, Neumann R, Bazavan R, Bazavan D and Antohe S 2008 *Physica E* **40** 2504
- [36] Simpkins B S, Pehrsson P E and Laracuente A R 2006 *Appl. Phys. Lett.* **88** 072111
- [37] Motayed A, Davydov A V, Mohammad S N and Melngailis J 2008 *J. Appl. Phys.* **104** 024302